Hif-1alpha induced expression of Il-1beta protects against mycobacterial infection in zebrafish.

[1,2]Nikolay V. Ogryzko, [1,3]Amy Lewis, [3]Heather L. Wilson, [4]Annemarie H. Meijer, [1,3]Stephen A. Renshaw and [1,3,]*Philip M. Elks

[1]The Bateson Centre, University of Sheffield, Western Bank, Sheffield, UK.

[2]MRC Centre for Inflammation Research, University of Edinburgh, Little France Crescent, Edinburgh, UK.

[3]Department of Infection and Immunity and Cardiovascular Disease, University of Sheffield, Western Bank, Sheffield, UK.

[4]Institute of Biology, Leiden University, Leiden, The Netherlands.

*Corresponding author:

Email: p.elks@sheffield.ac.uk (PME)

Running Title: Hif-1α induced il-1β protects against TB

Abstract

Drug resistant mycobacteria are a rising problem worldwide. There is an urgent need to understand the immune response to TB to identify host targets that, if targeted therapeutically, could be used to tackle these currently untreatable infections. Here, we use an Il-1β fluorescent transgenic line to show that there is an early innate immune pro-inflammatory response to well-established zebrafish models of inflammation and *Mycobacterium marinum* (Mm) infection. We demonstrate that host-derived hypoxia signalling, mediated by the Hif-1α transcription factor, can prime macrophages with increased levels of Il-1β in the absence of infection, upregulating neutrophil antimicrobial nitric oxide production, leading to greater protection against infection. Our data link Hif-1α to proinflammatory macrophage Il-1β transcription *in vivo* during early mycobacterial infection and importantly highlight a host protective mechanism, via antimicrobial nitric oxide, that decreases disease outcomes and that could be targeted therapeutically to stimulate the innate immune response to better deal with infections.

Keywords: Hif-1α/Il-1β/mycobacterium/hypoxia/zebrafish

Introduction

Pulmonary tuberculosis (TB) is a major world health problem caused by the bacillus *Mycobacterium tuberculosis* (*Mtb*) (World Health Organization, 2016). It is a current priority for infectious disease research due to increasing rates of multi- and totally-drug resistant strains causing high levels of mortality, especially in the immunocompromised (Koul *et al*, 2011). Mycobacteria are specialised at evading killing mechanisms of the immune system to survive. Mycobacteria and immune cells create a highly organised niche, called the granuloma, in which Mtb can proliferate or

enter a latent phase, protected from the immune system (Podinovskaia *et al*, 2013; Ramakrishnan, 2012). In human Mtb infection, bacteria first encounter cells of the innate immune system in and around the lungs, either macrophages in the alveolar space or neutrophils in the surrounding capillary vasculature, before the involvement of adaptive immunity and granuloma formation (Lerner *et al*, 2015; Jasenosky *et al*, 2015). These initial phagocytosis events are followed by the attraction of other innate immune cells which signal to draining lymph nodes to activate the adaptive immune response, signs of which only become apparent 3 to 8 weeks after infection in humans (Jasenosky *et al*, 2015). Although granuloma formation is reasonably well characterised, the initial interactions of the bacteria with the host innate immune cells are less well defined *in vivo*.

Mtb, like many other bacterial and pathogenic microbes, triggers a pro-inflammatory immune response via the activation of TLRs (Toll-like receptors) (Mortaz *et al*, 2015). The activation of the innate immune cells via TLR signalling is a critical early host response to many invading pathogens for successful clearance of infection and, in the absence of TLR signalling, mycobacteria grow unchecked to cause systemic infection (van der Vaart *et al*, 2013). Although mycobacteria can hijack host leukocytes to create a niche for their growth, in zebrafish models many of the initial Mm inoculum are neutralised by macrophages and neutrophils before infection can take hold (Hosseini *et al*, 2016; Cambier *et al*, 2013). Early mycobacterial interaction with host leukocytes is critical for the pathogen, and manipulation of the macrophage by the bacteria is required for establishment of a permissive niche in which the bacteria can grow and build its host derived protective structure, the granuloma (Meijer, 2016; Guirado *et al*, 2013). Indeed the control of the macrophage by Mm may happen early in infection, as there is a phase of infection from 6 hours to 1 day

post infection in the zebrafish model that is characterised by a dampening of the cytokine transcriptional response (Benard *et al*, 2016). Greater understanding of the diverse phenotype of macrophages immediately after infection may allow therapeutic tuning to provide maximal early control of mycobacteria during infection (McClean & Tobin, 2016; Dorhoi & Kaufmann, 2015). Recent studies in optically translucent zebrafish infection models have indicated that initial interactions between Mm and macrophages and neutrophils are more complex than originally thought, with successive rounds of bacterial internalisation and leukocyte cell death leading to granuloma formation (Hosseini *et al*, 2016; Cambier *et al*, 2017; Elks *et al*, 2015). The immune molecular mechanisms involved in these early processes are poorly understood.

We have previously demonstrated in a zebrafish/Mm model of TB that the initial immune response to infection can be enhanced by stabilising host-derived Hif-1α (hypoxia inducible factor-1 alpha), leading to reduced bacterial burden (Elks *et al*, 2013). Hif-1α is a major transcriptional regulator of the cellular response to hypoxia, that has been implicated in the activation of macrophages and neutrophils during infection and inflammatory processes (Cramer *et al*, 2003; Elks *et al*, 2011). Stabilisation of Hif-1α in zebrafish upregulated pro-inflammatory neutrophil nitric oxide (NO) production leading to lower mycobacterial burden (Elks *et al*, 2013, 2014a). The mechanisms by which pro-inflammatory cytokines associated with this NO increase are regulated by Hif-1α signalling is not known.

IL-1β is a critical macrophage-derived activator of immune cells with wide-ranging and complex effects on immune signalling and downstream pathways. IL-1β has been shown to be upregulated in the onset and formation of Mm and Mtb granulomas (Di Paolo *et al*, 2015; Bourigault *et al*, 2013; Novikov *et al*, 2011). We

hypothesised that IL-1β would be activated in specific immune cell populations early in Mm infection, (within 1-day post-infection, pre-granuloma formation) and that Hif-1α acts via altered expression of this important pro-inflammatory mediator to confer protection against mycobacterial infection. Here, using the zebrafish Mm model and fluorescent transgenic lines, we show that that *il-1β* is transcriptionally upregulated in macrophages early during *in vivo* infection. Stabilisation of Hif-1α upregulates *il-1β* transcription in macrophages in the absence of infection. *il-1β* signalling is required for protective NO production by neutrophils and a subsequent decrease in infection. Our data indicate that protective Hif-1α mediated NO is at least partially regulated by the key pro-inflammatory mediator Il-1β, increasing our understanding of the mechanism of action of the potential therapeutic target, Hif-1α, as a host-derived factor in TB.

Results

il-1β:GFP is upregulated in macrophages during early and later stage Mm infection

Il-1β is a major macrophage-derived pro-inflammatory cytokine that is upregulated in both inflammation and infection. The initial phase of Mm infection in zebrafish is characterised by a short period of greatly increased pro-inflammatory signalling (before 1 day post-infection, dpi) where the immune system reacts to Mm infection. This is followed by a lag-phase of decreased activity which allows for granuloma formation between 2-3dpi, before cytokine levels rise again in formed larval granulomas at 4dpi (Benard *et al*, 2016; Hosseini *et al*, 2016). However, the levels of pro-inflammatory cytokines have only been previously studied at a transcriptional

level in whole embryos or FACS sorted cells, rather than detecting levels *in situ*, over time, in an intact organism (Benard *et al*, 2016).

We hypothesised that Il-1β is a major pro-inflammatory cytokine that would be upregulated by both mycobacterial infection and Hif-1α stabilisation. We have previously shown upregulation of *il-1β* message after induction of inflammation via tailfin transection by qPCR and wholemount *in situ* hybridisation (WISH) in the zebrafish (Ogryzko *et al*, 2014a). *il-1β* is one of the most readily detectable pro-inflammatory cytokines during early granuloma stages of Mm infection and at 1 dpi (Figure 1A) (Van Der Vaart *et al*, 2014). At 1dpi transcription is upregulated 1.7 fold measured by qPCR, compared to PVP injection controls (Figure 1A). Macrophage expression of *il-1β* is greatly under-represented measured in this way on the wholebody level due to the small proportion of cells that contribute to the immune lineage. Therefore, to investigate *il-1β* expression on a cellular level *in vivo*, we developed a BAC (bacterial artificial chromosome) derived *il-1β* promoter driven GFP line, *TgBAC(il-1β:GFP)SH445*, to assess *il-1β* expression in real-time during mycobacterial infection. We sought to examine *il-1β:GFP* expression in our well-established inflammation assay before investigating its expression during mycobacterial infection. Both wholemount *in situ* hybridisation (WISH) of *il-1β* and *il-1β:GFP* do not exhibit any immune cell expression under basal conditions (Figure S1A-B and Figure 1B). *il-1β:GFP* recapitulates *il-1β* WISH expression in response to tail transection, with upregulation observed in cells in and around the caudal haematopoietic region (CHT), consistent with immune cell expression, (Figure S1A and B) (Ogryzko *et al*, 2014a), although, as expected, the synthesis of GFP occurs over a longer timescale than that of *il-1β* mRNA detected by WISH. Neutrophils are

the first cells to respond to tailfin transection with increased *il-1β:GFP*, with fluorescence first observed at 1hpw (hours post-wounding) and still present at 6hpw (Figure S1C). Having demonstrated that the il-1β:GFP is responsive to inflammation in similar cells over a similar timespan as the *in situ* hybridisation, we sought to investigate its regulation during mycobacterial infection.

We used the *TgBAC(il-1β:GFP)sh445* line to show that GFP is expressed in cells proximal to Mm infection sites at pre-granuloma phases (1dpi) (Figure 1B) and in larval granulomas (4dpi) (Figure 1C). Many of these cells contained Mm and had the appearance of activated immune cells with a dynamic branched phenotype (Figure 1B and Movie S1). The earliest timepoint at which *il-1β:GFP* could be detected by confocal microscopy was between 6 and 8 hours post infection, (Figure 2A), consistent with rapid transcriptional activation of the *il-1β* promoter after infection and similar to the timing of macrophage *il-1β:GFP* expression after tailfin transection (Figure 2B). *il-1β:GFP* was predominantly upregulated in infected macrophages at 1dpi (Figure 2C) consistent with their containment of phagocytosed Mm (Figure 1B). These data demonstrate that, during early stages of infection, *il-1β* is transcriptionally activated in infected macrophages as part of an early pro-inflammatory response.

Stabilisation of Hif-1α upregulates *il-1β:GFP* at early stages of infection

We have previously shown that stabilisation of Hif-1α induces neutrophil pro-inflammatory nitric oxide production (Elks *et al*, 2013, 2014a). We hypothesised that this may be a part of an increased pro-inflammatory profile in innate immune cells, therefore we tested whether Hif-1α is upregulating a pro-inflammatory program in the absence of infection using the *il-1β:GFP* transgenic line. Dominant active Hif-1α

significantly increased *il-1β:GFP* expression in the absence of Mm infection at 2dpf, while dominant negative Hif-1α caused no difference in *il-1β:GFP* expression (Figure 3A and B). These data indicate that *il-1β* expression is part of a pro-inflammatory response to increased Hif-1α levels that could aid the host response to Mm challenge.

Inhibition of *il-1β* increases Mm burden and inhibits the Hif-1α nitric oxide response

Il-1β is a major pro-inflammatory cytokine that in many infections is instrumental in coordinating the immune response (Cohen, 2014; Ogryzko *et al*, 2014b). We sought to test whether Il-1β was important in early Mm infection. When Il-1β was blocked using a well-characterised and validated *il-1β* morpholino, the morphants showed significantly increased infection compared to control morphants (Figure 4A and B).

We have previously shown that stabilisation of Hif-1α induces pro-inflammatory neutrophil nitric oxide production, via inducible nitric oxide synthase (iNOS) (Elks *et al*, 2013, 2014a). DA Hif-1α was not sufficient to reduce Mm infection levels when *il-1β* expression was blocked (Figure 4A and B) suggesting that the *il-1β* response to Mm infection is critical to control infection. These results were supported by generation of an *il-1β* null mutant ($il\text{-}1\beta^{SH446}$/ $il\text{-}1\beta^{SH446}$) (Figure S2), in which DA Hif-1α also did not decrease infection, while in wildtype siblings infection was reduced (Figure 4C and D).

NO production is found primarily in neutrophils after Mm infection in zebrafish larvae (Figure S3) (Elks *et al*, 2013, 2014b). We have previously demonstrated that inhibiting production of nitric oxide by Nos2 can block the antimicrobial effect of DA

198 Hif-1α (Elks *et al*, 2013). Blocking Il-1β production also significantly dampened the
199 neutrophil nitric oxide response after Mm infection at 1dpi (Figure 5A and B). As we
200 have previously observed, DA Hif-1α upregulated NO in the absence of infection
201 (PVP) an effect that is dampened by introduction of the bacteria (Mm) through
202 currently unknown mechanisms, (Figure 5C and D) (Elks *et al*, 2013). Here, we find
203 that *il-1β* MO blocked the increased production of nitrotyrosine by DA Hif-1α in the
204 absence of bacteria (PVP) (Figure 5C and D). These results show that Hif-1α
205 activation of Nos2 may, at least in part, be acting through *il-1β* activation (Figure 6)
206 and hint at a much more complex regulation of pro-inflammatory signalling by Hif-1α
207 than simply acting on Hif responsive elements (HREs) in the promoter of Nos2.
208
209 **Discussion**
210 Antimicrobial resistance is a rising problem in TB infections worldwide and there is
211 an urgent need to understand the regulation of host-immunity by TB so that we can
212 target host-derived factors to help tackle disease. Our data identify an early pro-
213 inflammatory response, involving macrophage *il-1β* expression, that is important for
214 the onset of early disease, but ultimately fails to control infection leading to
215 granuloma formation. Using a well-established zebrafish Mm model of TB, we show
216 that manipulation of Hif-1α can stimulate this pro-inflammatory network, aiding the
217 host fight against infection, moving towards early clearance of infection. Specifically,
218 we identify that Hif-1α driven Il-1β contributes to the NO response, a response we
219 have previously shown to be host protective (Elks *et al*, 2013, 2014a).
220 Here, we took advantage of a novel transgenic zebrafish line to understand the
221 dynamics and cell specificity of *il-1β* production in inflammation and mycobacterial
222 infection, with a focus on the understudied early stages (<1dpi) of the innate immune

response to TB infection. We confirmed that the *il-1β:GFP* expression of our line was faithful to *il-1β* transcription by following its expression in a well-characterised tailfin transection model of inflammation and comparison to *in situ* hybridisation data (Ogryzko *et al*, 2014a; Renshaw & Loynes, 2006). Furthermore, the expression pattern of our BAC transgenic line closely matches another recently published BAC promoter driven *il-1β* transgenic (Hasegawa *et al*, 2017). The *il-1β:GFP* line also displayed some GFP signal in muscle and epithelial cells in the tail. Similar GFP expression can be seen when driven by NF-kB response elements (Kanther *et al*, 2011) but not by WISH, suggesting this might be off-target expression resulting from the promoter region missing some negative regulatory elements, however, it could also be specific expression that is at too low a level to be detectable by *in situ* hybridisation. Although previous studies have shown *il-1β:GFP* to be upregulated in leukocytes at a tailfin transection (Hasegawa *et al*, 2017), we combined the *il-1β:GFP* line with leukocyte specific transgenics to show that neutrophils are the first to respond at the wound, with macrophages both migrating to and upregulating *il-1β:GFP* at later timepoints.

The Mtb granuloma is widely studied, both in terms of immunohistochemistry of human granulomas, and in mammalian models (Ulrichs & Kaufmann, 2006; Flynn *et al*, 2011; Via *et al*, 2008). These studies have demonstrated that the granuloma is rich in pro-inflammatory cytokine production. This pro-inflammatory environment has been observed in human TB, with IL-1β found to be in high levels in pleural fluid from TB patients with granulomas present (Orphanidou *et al*, 1996). Here we observe that the pro-inflammatory response is present at pre-granuloma stages. Lack of a pro-inflammatory response has been linked to poor treatment outcomes indicating that this host response is important even in the presence of antimycobacterial agents

(Waitt *et al*, 2015). The upregulation of proinflammatory cytokines in mycobacterial infection has also been shown in the zebrafish/Mm larval model of TB granulomas, but previous studies have mainly relied on immunohistochemistry and/or transcriptomics data from either wholebody larvae or FACs sorted immune cell populations (Benard *et al*, 2016; Marjoram *et al*, 2015). Using live cell imaging we found that *il-1β* transcription was upregulated at the granuloma formation stage, however we also demonstrated that it is upregulated before the granuloma stage within 6-8 hours hpi. Upon infection *il-1β:GFP* expression was predominantly upregulated in infected macrophages indicating that within the first 24 hours of infection there is a macrophage pro-inflammatory response. Murine and human cell studies have indicated that macrophages are able to produce IL-1β a few hours after mycobacterial challenge indicating that an early response is also present in mammalian systems, at least on a cellular level (Di Paolo *et al*, 2015; Robinson & Nau, 2008). Our observations are in line with our previous observation of Hif-1α signalling early after infection (detected using a *phd3:GFP* transgenic line), which was also observed in infected macrophages at 1dpi (Elks *et al*, 2013), indicating that *il-1β*, alongside Hif-1α signalling, is part of an immediate pro-inflammatory macrophage response. As with Hif-1α, our data indicate that Mm triggered *il-1β* is not sufficient to control infection with subsequent widespread granuloma formation at later stages, however if primed with high *il-1β* and NO via Hif-1α the immune response is boosted leading to lower infection, towards early infection clearance.

We have previously demonstrated that stabilisation of Hif-1α can aid the zebrafish host to control Mm infection, at least in part by priming neutrophils with increased nitrotyrosine generated by the Nos2 enzyme (Elks *et al*, 2013). If the Nos2 enzyme is blocked either pharmacologically or genetically the protective effect of Hif-1α

stabilisation is lost (Elks *et al*, 2013). Here, we show that stabilisation of Hif-1α upregulates pro-inflammatory macrophage *il-1β* expression in the absence of an infection challenge. If Il-1β activity is repressed then Hif-1α induced reduction in bacterial burden is abrogated, alongside the Hif-1α dependent increase in NO production. These data show regulation of both Nos2 and Il-1β by Hif-1α, and that Hif-1α driven NO production is partially dependent on Il-1β induction. Both human NOS-2 and IL-1β have HREs (HIF responsive elements) in their promoters and direct regulation by HIF-α signalling has been previously demonstrated *in vitro* (Zhang *et al*, 2006; Charbonneau *et al*, 2007). The link between HIF-1α and IL-1β has been previously demonstrated in murine macrophages via inflammatory activation by succinate, in the absence of infection (Tannahill *et al*, 2013). In a murine model of *Mycobacterium tuberculosis* it was found that HIF-1α is critical for IFN-γ–dependent control of M. tuberculosis infection, but it has not previously been demonstrated that HIF-1α is important for innate defense of macrophages against M. tuberculosis (Braverman *et al*, 2016). Our data do not rule out direct regulation of Nos2 by Hif-1α, as blocking Il-1β is likely to have wider spread immune effects, however they do suggest that Nos2 is partially upregulated by Il-1β in the stabilised Hif-1α context. These observations, alongside our finding that blocking Il-1β, primarily observed in macrophages, can block Hif-1α induced neutrophil nitrotyrosine production, indicate a close interplay between macrophages and neutrophils during early mycobacterial infection that is not yet fully understood.

IL-1β is an important pro-inflammatory component and is one of the cytokines that has been shown to be transcriptionally depressed during the 6 hour to 1dpi period of Mm/zebrafish pathogenesis (Benard *et al*, 2016). Although this depression was not

297 detectable using the *il-1β:GFP* line, presumably due to the early transcriptional
298 response post-infection coupled with the stability of the GFP protein, our data
299 indicate that increased *il-1β* transcription due to Hif-1α stabilisation during this early
300 stage of Mm infection is protective to the host. Alongside transcription, the
301 processing of Il-1β by caspases plays a crucial role in immune cell pyroptosis
302 mediated by the inflammasome (Malik & Kanneganti, 2017). Recent findings in the
303 Mm/zebrafish model indicate that neutrophils and macrophages can efficiently
304 phagocytose bacteria and undergo rounds of cell death and re-uptake during the
305 initial days of infection (Hosseini *et al*, 2016). Although here we show a role for early
306 pro-inflammatory *il-1β* transcription during Mm infection, the role of Il-1β processing
307 and inflammasome induced pyroptosis/cell death in these early Mm immune
308 processes remain undetermined.
309 In conclusion, our data demonstrate an early pro-inflammatory response of Mm
310 infected macrophages *in vivo*. By stabilising Hif-1α, macrophage Il-1β can be primed
311 in the absence of infection and is protective upon Mm infection via neutrophil nitric
312 oxide production. Therapeutic strategies targeting these signalling mechanisms
313 could decrease the level of initial mycobacteria in patients and act to block the
314 development of active TB by reactivation of macrophage pro-inflammatory stimuli.
315 Furthermore, our findings may have important implications in other human infectious
316 diseases in which the pathogen is able to circumvent the proinflammatory immune
317 response to allow its survival and proliferation. Therapies that target host-derived
318 signalling pathways such as these would be beneficial against multidrug resistant
319 strains and could act to shorten the currently long antibiotic therapies required to
320 clear TB from patients.
321

Materials and Methods

Zebrafish and bacterial strains

Zebrafish were raised and maintained on a 14:10-hour light/dark cycle at 28 degrees C, according to standard protocols (Nusslein-Volhard C, 2002), in UK Home Office approved facilities at The Bateson Centre aquaria at the University of Sheffield. Strains used were Nacre (wildtype), *Tg(mpeg1:mCherry-F)ump2Tg, TgBAC(il-1β:eGFP)sh445* *Tg(mpeg1:mCherryCAAX)sh378* and *Tg(lyz:Ds-RED2)nz50* (Marjoram *et al*, 2015; Bojarczuk *et al*, 2016; Nguyen-Chi *et al*, 2015; Hall *et al*, 2007).

Mm infection experiments were performed using M. marinum M (ATCC #BAA-535), containing a psMT3-mCherry or psMT3 mCrimson vector (van der Sar *et al*, 2009). Injection inoculum was prepared from an overnight liquid culture in the log-phase of growth resuspended in 2% polyvinylpyrrolidone40 (PVP40) solution (CalBiochem) as previously described (Cui *et al*, 2011). 100-150 colony forming units (CFU) were injected into the caudal vein at 28-30hpf as previously described (Benard *et al*, 2012).

Generation of *TgBAC(il-1α:GFP)sh445* transgenic and *il-1β*^{SH446}/ *il-1β*^{SH446} mutant zebrafish

An eGFP SV40 polyadenylation cassette inserted at the *il-1β* ATG start site of zebrafish BAC CH-211-147h23 using established protocols (Renshaw *et al*, 2006). Inverted Tol2 elements were inserted into the chloramphenicol coding sequence and the resulting modified BAC was used to generate *TgBAC(il-1β:eGFP)sh445*.

346 *il-1-/-* (*il-1β*^{SH446}/*il-1β*^{SH446}) mutant embryos were generated by CRISPR-Cas9
347 mediated mutagenesis targeted around an Mwo1 restriction site in the third exon of
348 *il-1β* using the method described by Hruscha et al (2013) and the template sequence
349 5'-
350 AAAGCACCGACTCGGTGCCACTTTTTCAAGTTGATAACGGACTAGCCTTATTTTA
351 ACTTGCTATTTCTAGCTCTAAAAC**TGAGCATGTCCAGCACCTC**GGCTATAGTGA
352 GTCGTATTACGC-3' (*il-1β* target sequence in bold). PCR with il-1gF 5'-
353 TAAGGAAAAACTCACTTC-3' and il-1gR 5'ATACGTGGACATGCTGAA3' and
354 subsequent Mwo1 digestion were used for genotyping.
355

356 **Morpholino knockdown of *il-1β***

357 The *il-1bβ* morpholino (Genetools) was used as previously reported (López-Muñoz *et*
358 *al*, 2011). A standard control morpholino (Genetools) was used as a negative
359 control.
360

361 **Confocal microscopy of transgenic larvae**

362 1dpi and 4dpi transgenic zebrafish larvae infected with fluorescent Mm strains were
363 mounted in 0.8-1% low melting point agarose (Sigma-Aldrich) and imaged on a Leica
364 TCS-SPE confocal on an inverted Leica DMi8 base and imaged using 20x or 40x
365 objective lenses.
366 For quantification purposes acquisition settings and area of imaging (in the caudal
367 vein region) were kept the same across groups. Corrected total cell fluorescence
368 was calculated for each immune-stained cell using Image J as previously described
369 (Elks *et al*, 2013, 2014a).
370

371 **Tailfin transection**

372 Inflammation was induced in zebrafish embryos by tail transection at 2 or 3dpf as
373 described previously (Renshaw & Loynes, 2006). Embryos were anesthetised by
374 immersion in 0.168 mg/mL Tricaine (Sigma-Aldrich), and tail transection was
375 performed using a microscalpel (World Precision Instruments).

376

377 **qPCR of *il-1β***

378 SYBR green qPCR was performed on 1dpi Mm infected (or PVP control) embryos as
379 previously described (Van Der Vaart *et al*, 2014). The following primers were used:
380 *il-1β*, accession number NM_212844, forward primer:
381 GAACAGAATGAAGCACATCAAACC, reverse primer:
382 ACGGCACTGAATCCACCAC, *ppial* control, accession number AY391451, forward
383 primer: ACACTGAAACACGGAGGCAAG, reverse primer:
384 CATCCACAACCTTCCCGAACAC.

385

386 **Bacterial pixel count**

387 Mm mCherry infected zebrafish larvae were imaged at 4dpi on an inverted Leica
388 DMi8 with a 2.5x objective lens. Brightfield and fluorescent images were captured
389 using a Hammamatsu OrcaV4 camera. Bacterial burden was assessed using
390 dedicated pixel counting software as previously described (Stoop *et al*, 2011).

391

392 **RNA injections**

393 Embryos were injected with dominant *hif-1αb* variant RNA at the one cell stage as
394 previously described (Elks *et al*, 2011). *hif-1α* variants used were dominant active

(DA) and dominant negative (DN) *hif-1α* (ZFIN: *hif1ab*). Phenol red (PR) (Sigma Aldrich) was used as a vehicle control.

Anti-nitrotyrosine antibody staining

Larvae were fixed in 4% paraformaldehyde in PBS overnight at 4°C and nitrotyrosine levels were immune-labelled using a rabbit polyclonal anti-nitrotyrosine antibody (Merck Millipore 06-284) and were detected using an Alexa Fluor conjugated secondary antibody (Invitrogen Life Technologies) as previously described (Elks *et al*, 2013, 2014a).

Statistical analysis

All data were analysed (Prism 7.0, GraphPad Software) using unpaired, two-tailed t-tests for comparisons between two groups and one-way ANOVA (with Bonferonni post-test adjustment) for other data. P values shown are: **P* < .05, ***P* < .01, and ****P* < .001.

Funding

This work was supported by a Sir Henry Dale Fellowship jointly funded by the Wellcome Trust and the Royal Society (grant number 105570/Z/14/Z) awarded to (P.M.E.). (S.A.R.) is funded by an MRC Programme Grant (MR/M004864/1). (A.H.M.) is funded by a Smart Mix Program of the Netherlands Ministry of Economic Affairs and the Ministry of Education, Culture and Science. (N.V.O. and H.L.W.) are funded by British Heart Foundation (BHF) project grant (PG/13/80/30443) and

Biotechnology and Biological Sciences Research Council (BBSRC) project grant (BB/L000830/1).

Acknowledgements

The authors would like to thank the Bateson Centre Aquarium Team at the University of Sheffield for fish care. We gratefully thank Georges Lutfalla (Montpellier University) for providing the *Tg(mpeg1:mCherry-F)ump2Tg line,* Lalita Ramakrishnan (University of Washington, Seattle) for M. marinum strains and Astrid van der Sar (VU University Medical Center, Amsterdam) for the pSMT3-mCherry vector.

Author Contributions

Conceived and designed the experiments: PME, SAR, NVO. Performed the experiments: PME, NVO, AL. Analysed the data: PME, NVO, HW, AHM, SAR. Wrote the paper: PME, NVO, SAR.

Conflict of Interest

The authors declare that they have no conflict of interest.

Benard EL, Rougeot J, Racz PI, Spaink HP & Meijer AH (2016) Transcriptomic Approaches in the Zebrafish Model for Tuberculosis—Insights Into Host- and Pathogen-specific Determinants of the Innate Immune Response. *Adv. Genet.* **95:** 217–251

Benard EL, van der Sar AM, Ellett F, Lieschke GJ, Spaink HP & Meijer AH (2012) Infection of zebrafish embryos with intracellular bacterial pathogens. *J Vis Exp* Available at: http://www.ncbi.nlm.nih.gov/pubmed/22453760

444 Bojarczuk A, Miller KA, Hotham R, Lewis A, Ogryzko N V., Kamuyango AA, Frost H, Gibson
445 RH, Stillman E, May RC, Renshaw SA & Johnston SA (2016) Cryptococcus neoformans
446 Intracellular Proliferation and Capsule Size Determines Early Macrophage Control of
447 Infection. *Sci. Rep.* **6:** 21489 Available at: http://www.nature.com/articles/srep21489
448 Bourigault M-L, Segueni N, Rose S, Court N, Vacher R, Vasseur V, Erard F, Le Bert M, Garcia I,
449 Iwakura Y, Jacobs M, Ryffel B & Quesniaux VFJ (2013) Relative contribution of IL-1α, IL-
450 1β and TNF to the host response to Mycobacterium tuberculosis and attenuated M.
451 bovis BCG. *Immunity, Inflamm. Dis.* **1:** 47–62 Available at:
452 http://www.pubmedcentral.nih.gov/articlerender.fcgi?artid=4217540&tool=pmcentrez
453 &rendertype=abstract
454 Braverman J, Sogi KM, Benjamin D, Nomura DK & Stanley SA (2016) HIF-1α Is an Essential
455 Mediator of IFN-γ–Dependent Immunity to *Mycobacterium tuberculosis*. *J. Immunol.*
456 **197:** 1287–1297 Available at:
457 http://www.jimmunol.org/lookup/doi/10.4049/jimmunol.1600266
458 Cambier CJ, O'Leary SM, O'Sullivan MP, Keane J & Ramakrishnan L (2017) Phenolic
459 Glycolipid Facilitates Mycobacterial Escape from Microbicidal Tissue-Resident
460 Macrophages. *Immunity*
461 Cambier CJ, Takaki KK, Larson RP, Hernandez RE, Tobin DM, Urdahl KB, Cosma CL &
462 Ramakrishnan L (2013) Mycobacteria manipulate macrophage recruitment through
463 coordinated use of membrane lipids. *Nature* **505:** 218–222 Available at:
464 http://www.nature.com/doifinder/10.1038/nature12799
465 Charbonneau M, Harper K, Grondin F, Pelmus M, McDonald PP & Dubois CM (2007)
466 Hypoxia-inducible factor mediates hypoxic and tumor necrosis factor alpha-induced
467 increases in tumor necrosis factor-alpha converting enzyme/ADAM17 expression by

468 synovial cells. *J. Biol. Chem.* **282:** 33714–24 Available at:
469 http://www.jbc.org/content/282/46/33714.full
470 Cohen P (2014) The TLR and IL-1 signalling network at a glance. *J. Cell Sci.* **127:** 2383–2390
471 Available at: http://jcs.biologists.org/cgi/doi/10.1242/jcs.149831
472 Cramer T, Yamanishi Y, Clausen BE, Forster I, Pawlinski R, Mackman N, Haase VH, Jaenisch R,
473 Corr M, Nizet V, Firestein GS, Gerber HP, Ferrara N & Johnson RS (2003) HIF-1alpha is
474 essential for myeloid cell-mediated inflammation. *Cell* **112:** 645–657 Available at:
475 http://www.ncbi.nlm.nih.gov/pubmed/12628185
476 Cui C, Benard EL, Kanwal Z, Stockhammer OW, van der Vaart M, Zakrzewska A, Spaink HP &
477 Meijer AH (2011) Infectious disease modeling and innate immune function in zebrafish
478 embryos. *Methods Cell Biol* **105:** 273–308 Available at:
479 http://www.ncbi.nlm.nih.gov/pubmed/21951535
480 Dorhoi A & Kaufmann SHE (2015) Versatile myeloid cell subsets contribute to tuberculosis-
481 associated inflammation. *Eur. J. Immunol.* **45:** 2191–2202
482 Elks PM, Brizee S, van der Vaart M, Walmsley SR, van Eeden FJ, Renshaw SA & Meijer AH
483 (2013) PLOS Pathogens: Hypoxia Inducible Factor Signaling Modulates Susceptibility to
484 Mycobacterial Infection via a Nitric Oxide Dependent Mechanism. *PLoS Pathog.* **9:**
485 e1003789 Available at:
486 http://www.plospathogens.org/article/info%3Adoi%2F10.1371%2Fjournal.ppat.10037
487 89%5Cnpapers2://publication/doi/10.1371/journal.ppat.1003789
488 Elks PM, van Eeden FJ, Dixon G, Wang X, Reyes-Aldasoro CC, Ingham PW, Whyte MK,
489 Walmsley SR & Renshaw SA (2011) Activation of hypoxia-inducible factor-1alpha (Hif-
490 1alpha) delays inflammation resolution by reducing neutrophil apoptosis and reverse
491 migration in a zebrafish inflammation model. *Blood* **118:** 712–722 Available at:

492 http://www.ncbi.nlm.nih.gov/pubmed/21555741

493 Elks PM, Renshaw SA, Meijer AH, Walmsley SR & van Eeden FJ (2015) Exploring the HIFs,
494 buts and maybes of hypoxia signalling in disease: lessons from zebrafish models. *Dis.*
495 *Model. Mech.* **8:** 1349–1360 Available at:
496 http://dmm.biologists.org/cgi/doi/10.1242/dmm.021865

497 Elks PM, Van Der Vaart M, Van Hensbergen V, Schutz E, Redd MJ, Murayama E, Spaink HP &
498 Meijer AH (2014a) Mycobacteria counteract a TLR-mediated nitrosative defense
499 mechanism in a zebrafish infection model. *PLoS One* **9:**

500 Elks PM, Van Der Vaart M, Van Hensbergen V, Schutz E, Redd MJ, Murayama E, Spaink HP &
501 Meijer AH (2014b) Mycobacteria counteract a TLR-mediated nitrosative defense
502 mechanism in a zebrafish infection model. *PLoS One* **9:**

503 Flynn JL, Chan J & Lin PL (2011) Macrophages and control of granulomatous inflammation in
504 tuberculosis. *Mucosal Immunol* **4:** 271–278 Available at:
505 http://www.ncbi.nlm.nih.gov/pubmed/21430653

506 Guirado E, Schlesinger LS & Kaplan G (2013) Macrophages in tuberculosis: Friend or foe.
507 *Semin. Immunopathol.* **35:** 563–583

508 Hall C, Flores M V, Storm T, Crosier K & Crosier P (2007) The zebrafish lysozyme C promoter
509 drives myeloid-specific expression in transgenic fish. *BMC Dev Biol* **7:** 42 Available at:
510 http://www.ncbi.nlm.nih.gov/pubmed/17477879

511 Hasegawa T, Hall CJ, Crosier PS, Abe G, Kawakami K, Kudo A & Kawakami A (2017) Transient
512 inflammatory response mediated by interleukin-1β is required for proper regeneration
513 in zebrafish fin fold. *Elife* **6:**

514 Hosseini R, Lamers GEM, Soltani HM, Meijer AH, Spaink HP & Schaaf MJM (2016)
515 Efferocytosis and extrusion of leukocytes determine the progression of early

516 mycobacterial pathogenesis. *J. Cell Sci.* **129:** 3385–3395 Available at:
517 http://jcs.biologists.org/lookup/doi/10.1242/jcs.135194
518 Jasenosky LD, Scriba TJ, Hanekom WA & Goldfeld AE (2015) T cells and adaptive immunity to
519 Mycobacterium tuberculosis in humans. *Immunol. Rev.* **264:** 74–87
520 Kanther M, Sun X, Mhlbauer M, MacKey LC, Flynn EJ, Bagnat M, Jobin C & Rawls JF (2011)
521 Microbial colonization induces dynamic temporal and spatial patterns of NF-??B
522 activation in the zebrafish digestive tract. *Gastroenterology* **141:** 197–207
523 Koul A, Arnoult E, Lounis N, Guillemont J & Andries K (2011) The challenge of new drug
524 discovery for tuberculosis. *Nature* **469:** 483–490 Available at:
525 http://www.nature.com/doifinder/10.1038/nature09657
526 Lerner TR, Borel S & Gutierrez MG (2015) The innate immune response in human
527 tuberculosis. *Cell. Microbiol.* **17:** 1277–1285
528 López-Muñoz A, Sepulcre MP, Roca FJ, Figueras A, Meseguer J & Mulero V (2011)
529 Evolutionary conserved pro-inflammatory and antigen presentation functions of
530 zebrafish IFN?? revealed by transcriptomic and functional analysis. *Mol. Immunol.* **48:**
531 1073–1083
532 Malik A & Kanneganti T-D (2017) Inflammasome activation and assembly at a glance. *J. Cell*
533 *Sci.* **130:** 3955–3963 Available at:
534 http://jcs.biologists.org/lookup/doi/10.1242/jcs.207365
535 Marjoram L, Alvers A, Deerhake ME, Bagwell J, Mankiewicz J, Cocchiaro JL, Beerman RW,
536 Willer J, Sumigray KD, Katsanis N, Tobin DM, Rawls JF, Goll MG & Bagnat M (2015)
537 Epigenetic control of intestinal barrier function and inflammation in zebrafish. *Proc.*
538 *Natl. Acad. Sci. U. S. A.* **112:** 2770–5 Available at:
539 www.ncbi.nlm.nih.gov/pubmed/25730872

McClean CM & Tobin DM (2016) Macrophage form, function, and phenotype in mycobacterial infection: Lessons from tuberculosis and other diseases. *Pathog. Dis.* **74:**

Meijer AH (2016) Protection and pathology in TB: learning from the zebrafish model. *Semin. Immunopathol.* **38:** 261–273

Mortaz E, Adcock IM, Tabarsi P, Masjedi MR, Mansouri D, Velayati AA, Casanova JL & Barnes PJ (2015) Interaction of Pattern Recognition Receptors with Mycobacterium Tuberculosis. *J. Clin. Immunol.* **35:**

Nguyen-Chi M, Laplace-Builhe B, Travnickova J, Luz-Crawford P, Tejedor G, Phan QT, Duroux-Richard I, Levraud JP, Kissa K, Lutfalla G, Jorgensen C & Djouad F (2015) Identification of polarized macrophage subsets in zebrafish. *Elife* **4:**

Novikov A, Cardone M, Thompson R, Shenderov K, Kirschman KD, Mayer-Barber KD, Myers TG, Rabin RL, Trinchieri G, Sher A & Feng CG (2011) Mycobacterium tuberculosis triggers host type I IFN signaling to regulate IL-1β production in human macrophages. *J. Immunol.* **187:** 2540–7 Available at: http://www.ncbi.nlm.nih.gov/pubmed/21784976%5Cnhttp://www.pubmedcentral.nih.gov/articlerender.fcgi?artid=PMC3159798

Nusslein-Volhard C DR (2002) Zebrafish: A Practical Approach 1st ed. Oxford: Oxford University Press

Ogryzko N V., Hoggett EE, Solaymani-Kohal S, Tazzyman S, Chico TJA, Renshaw SA & Wilson HL (2014a) Zebrafish tissue injury causes upregulation of interleukin-1 and caspase-dependent amplification of the inflammatory response. *Dis. Model. Mech.* **7:** 259–264 Available at: http://dmm.biologists.org/cgi/doi/10.1242/dmm.013029

Ogryzko N V., Renshaw SA & Wilson HL (2014b) The IL-1 family in fish: Swimming through the muddy waters of inflammasome evolution. *Dev. Comp. Immunol.* **46:** 53–62

564 Orphanidou D, Gaga M, Rasidakis A, Dimakou K, Toumbis M, Latsi P, Pandalos J,
565 Christacopoulou J & Jordanoglou J (1996) Tumour necrosis factor, interleukin-1 and
566 adenosine deaminase in tuberculous pleural effusion. *Respir. Med.* **90:** 95–98
567 Di Paolo NC, Shafiani S, Day T, Papayannoupoulou T, Russell DW, Iwakura Y, Sherman D,
568 Urdahl K & Shayakhmetov DM (2015) Interdependence between Interleukin-1 and
569 Tumor Necrosis Factor Regulates TNF-Dependent Control of Mycobacterium
570 tuberculosis Infection. *Immunity* **43:** 1125–1136 Available at:
571 http://www.sciencedirect.com/science/article/pii/S107476131500494X%5Cnhttp://w
572 ww.sciencedirect.com/science/article/pii/S107476131500494X/pdfft?md5=b6007f686
573 c768807c7cd489777f7ab49&pid=1-s2.0-S107476131500494X-
574 main.pdf%5Cnhttp://linkinghub.elsevier.com/ret
575 Podinovskaia M, Lee W, Caldwell S & Russell DG (2013) Infection of macrophages with
576 Mycobacterium tuberculosis induces global modifications to phagosomal function. *Cell.*
577 *Microbiol.* **15:** 843–859
578 Ramakrishnan L (2012) Revisiting the role of the granuloma in tuberculosis. *Nat. Rev.*
579 *Immunol.* Available at: http://www.nature.com/doifinder/10.1038/nri3211
580 Renshaw S & Loynes C (2006) A transgenic zebrafish model of neutrophilic inflammation.
581 *Blood…* **108:** 3976–3978 Available at:
582 http://bloodjournal.hematologylibrary.org/content/108/13/3976.short
583 Renshaw SA, Loynes CA, Trushell DM, Elworthy S, Ingham PW & Whyte MK (2006) A
584 transgenic zebrafish model of neutrophilic inflammation. *Blood* **108:** 3976–3978
585 Available at: http://www.ncbi.nlm.nih.gov/pubmed/16926288
586 Robinson CM & Nau GJ (2008) Interleukin-12 and interleukin-27 regulate macrophage
587 control of Mycobacterium tuberculosis. *J. Infect. Dis.* **198:** 359–366

588 van der Sar AM, Spaink HP, Zakrzewska A, Bitter W & Meijer AH (2009) Specificity of the
589 zebrafish host transcriptome response to acute and chronic mycobacterial infection
590 and the role of innate and adaptive immune components. *Mol Immunol* **46:** 2317–2332
591 Available at: http://www.ncbi.nlm.nih.gov/pubmed/19409617
592 Stoop EJ, Schipper T, Huber SK, Nezhinsky AE, Verbeek FJ, Gurcha SS, Besra GS,
593 Vandenbroucke-Grauls CM, Bitter W & van der Sar AM (2011) Zebrafish embryo screen
594 for mycobacterial genes involved in the initiation of granuloma formation reveals a
595 newly identified ESX-1 component. *Dis Model Mech* **4:** 526–536 Available at:
596 http://www.ncbi.nlm.nih.gov/pubmed/21372049
597 Tannahill GM, Curtis AM, Adamik J, Palsson-Mcdermott EM, McGettrick AF, Goel G, Frezza
598 C, Bernard NJ, Kelly B, Foley NH, Zheng L, Gardet A, Tong Z, Jany SS, Corr SC, Haneklaus
599 M, Caffrey BE, Pierce K, Walmsley S, Beasley FC, et al (2013) Succinate is an
600 inflammatory signal that induces IL-1β through HIF-1α. *Nature* **496:** 238–242
601 Ulrichs T & Kaufmann SH (2006) New insights into the function of granulomas in human
602 tuberculosis. *J Pathol* **208:** 261–269 Available at:
603 http://www.ncbi.nlm.nih.gov/pubmed/16362982
604 Van Der Vaart M, Korbee CJ, Lamers GEM, Tengeler AC, Hosseini R, Haks MC, Ottenhoff
605 THM, Spaink HP & Meijer AH (2014) The DNA damage-regulated autophagy modulator
606 DRAM1 links mycobacterial recognition via TLP-MYD88 to authophagic defense. *Cell*
607 *Host Microbe* **15:** 753–767
608 van der Vaart M, van Soest JJ, Spaink HP & Meijer AH (2013) Functional analysis of a
609 zebrafish myd88 mutant identifies key transcriptional components of the innate
610 immune system. *Dis. Model. Mech.* Available at:
611 http://www.ncbi.nlm.nih.gov/pubmed/23471913

612 Via LE, Lin PL, Ray SM, Carrillo J, Allen SS, Eum SY, Taylor K, Klein E, Manjunatha U, Gonzales
613 J, Lee EG, Park SK, Raleigh JA, Cho SN, McMurray DN, Flynn JL & Barry 3rd CE (2008)
614 Tuberculous granulomas are hypoxic in guinea pigs, rabbits, and nonhuman primates.
615 *Infect Immun* **76:** 2333–2340 Available at:
616 http://www.ncbi.nlm.nih.gov/pubmed/18347040
617 Waitt CJ, Banda P, Glennie S, Kampmann B, Squire SB, Pirmohamed M & Heyderman RS
618 (2015) Monocyte unresponsiveness and impaired IL1β, TNFα and IL7 production are
619 associated with a poor outcome in Malawian adults with pulmonary tuberculosis. *BMC*
620 *Infect. Dis.* **15:** 513 Available at: http://www.biomedcentral.com/1471-2334/15/513
621 World Health Organization (2016) Multidrug-Resistant Tuberculosis (MDR-TB). *Burden, Glob.*
622 *Treat. Enroll. O N Mdr-tb Outcomes, Treat.*: 2015–2016
623 Zhang W, Petrovic JM, Callaghan D, Jones A, Cui H, Howlett C & Stanimirovic D (2006)
624 Evidence that hypoxia-inducible factor-1 (HIF-1) mediates transcriptional activation of
625 interleukin-1?? (IL-1??) in astrocyte cultures. *J. Neuroimmunol.* **174:** 63–73

626

627 **Figure Legends**

628

629 **Figure 1. *TgBAC(il-1β:GFP)sh445* is upregulated by Mm in infected**
630 **macrophages at early and later stage infection**

631 A) Graph showing relative wholebody *il-1β* mRNA expression by SYBRgreen qPCR
632 in Mm infected 1dpi larvae (Mm) and mock injected controls (PVP). Data shown are
633 mean ± SEM, n=3 independent experiments.
634 (B) Fluorescent confocal micrographs of 1dpi larvae, prior to granuloma formation.
635 Unchallenged *TgBAC(il-1β:GFP)sh445* has no detectable expression in immune

cells and low detectable levels in the yolk (dotted line) and some muscle cells. *il-1β* expression was detected by GFP levels, in green, using the *TgBAC(il-1:eGFP)sh445* transgenic line. Mm mCherry is shown in the red channel. Increased levels of *il-1β:GFP* expression were detectable in cells associated with infection. Infected macrophages with *il-1β-GFP* levels have an activated, branched phenotype (white arrowheads).

(C) Fluorescent confocal micrographs of 4dpi larvae. *il-1β* expression was detected by GFP levels, in green, using the *TgBAC(il-1:eGFP)sh445* transgenic line. Mm mCherry is shown in the red channel. Increased levels of *il-1β:GFP* expression were detectable in immune cells that are in the blood vessels (Ci and blown up in Ciii, blood vessel indicated by solid white lines) and in early tissue granulomas (Cii and blown up in Civ).

Figure 2. *il-1β:GFP* is activated 6-8 hours after challenge in macrophages.

(A) Fluorescent confocal micrographs of a timelapse between 6 to 8 hours post Mm infection. Mm mCherry is shown in the red channel and *il-1β:GFP* in the green channel with the microscope settings set to detect low GFP levels. Arrowheads indicate the emergence of *il-1β:GFP* expression in an infected cell.

(B) Fluorescent confocal micrographs of *TgBAC(il-1β:GFP)sh445* crossed to *Tg(mpeg1:mCherryCAAX)sh378* line labelling macrophages. The tailfin was transected at 3dpf and fluorescence imaging was performed at the wound at 1 hour post wound (1hpw) and 6hpw. Red macrophages are not positive for *il-1β:GFP* expression at 1hpw and the first detectable *il-1β:GFP* expression is found in the macrophages at 6hpw.

(C) Fluorescent confocal micrographs of 1dpi caudal vein region of infection. *il-1β* expression was detected by GFP levels, in green, using the *TgBAC(il-1β:eGFP)sh445* transgenic line. Macrophages are shown in red using a *Tg(mpeg1:mCherryCAAX)sh378* line. Mm Crimson is shown in the blue channel (right panels) with a PVP control (left panels). Without infection there is little overlap of *il-1β:GFP* and *mpeg:mCherry*, while in infected larvae macrophages have higher levels of *il-1β:GFP*. Arrowheads indicate infected macrophages with high levels of *il-1β:GFP.* Dotted lines indicate the yolk extension of the larvae where there is non-specific fluorescence.

Figure 3. *il-1β:GFP* is upregulated in the absence of infection by DA Hif-1α

(A) Fluorescent confocal micrographs of 1dpi caudal vein region of infection. *il-1β:GFP* expression was detected by GFP levels, in green, using the *TgBAC(il-1:eGFP)sh445* transgenic line. Larvae were injected at the 1 cell stage with dominant negative (DN) or dominant active (DA) Hif-1α or phenol red (PR) control. Non-infected larvae are in the left panels (PVP) and Mm Crimson infected larvae are in the right panels (Mm). Dotted lines indicate the yolk extension of the larvae where there is non-specific fluorescence.

(B) Corrected fluorescence intensity levels of *il-1β:GFP* confocal z-stacks in uninfected larvae (PVP, empty bars) and infected larvae (Mm, filled bars) at 1dpi. Dominant active Hif-1α (DA1) had significantly increased *il-1β:GFP* levels in the absence of Mm bacterial challenge compared to phenol red (PR) and dominant negative Hif-1α (DN1) injected controls. Data shown are mean ± SEM, n=24-48 cells from 4-8 embryos representative of 3 independent experiments.

Figure 4. *il-1β* knockdown abrogates the protective effect of DA Hif-1α on bacterial burden

(A) Stereo-fluorescence micrographs of Mm mCherry infected 4dpi larvae after injection with DA Hif-1α (DA1) and the *il-1β* morpholino (Il-1 MO), using the standard control morpholino and phenol red (Control) as a negative control.

(B) Bacterial burden of larvae shown in (A). Data shown are mean ± SEM, n=46-50 as accumulated from 3 independent experiments.

(C) Stereo-fluorescence micrographs of Mm mCherry infected 4dpi larvae of *il-1β* knockout (il-1-/-) and sibling wildtype controls (WT) after injection of DA Hif-1α (DA1) or phenol red (PR) as a negative control.

(D) Bacterial burden of larvae shown in (C). Data shown are mean ± SEM, n=16-20 as accumulated from 3 independent experiments.

Figure 5. *il-1β* knockdown abrogates DA Hif-1α dependent nitrotyrosine production

(A) Example fluorescence confocal z-stacks of the caudal vein region of embryos stained with Alexa-633 labelled anti-nitrotyrosine antibody (red), imaged at 1dpi in the presence or absence of Mm infection. One-cell stage embryos were injected with phenol red (PR). One-cell stage embryos we co-injected with *il-1β* morpholino or (il-1 MO) or standard control morpholino (Cont MO). At 1dpi larvae were either infected with Mm mCherry (Mm), or PVP as a non-infected control (Mm channel not shown in these panels).

(B) Example fluorescence confocal z-stacks of the caudal vein region of embryos stained with Alexa-633 labelled anti-nitrotyrosine antibody (red), imaged at 1dpi in the presence or absence of Mm infection. One-cell stage embryos were injected with dominant active Hif-1α (DA). One-cell stage embryos we co-injected with *il-1β* morpholino or (il-1 MO) or standard control morpholino (Cont MO). At 1dpi larvae were either infected with Mm mCherry (Mm), or PVP as a non-infected control (Mm channel not shown in these panels).

(C) Corrected fluorescence intensity levels of anti-nitrotyrosine antibody confocal z-stacks of phenol red (PR) control injected embryos in the presence or absence of Mm infection at 1dpi. Control morpholino is shown in the clear bars and *il-1β* morpholino (il-1 MO) in the filled bars. Data shown are mean ± SEM, n=54-59 cells from 10-12 embryos accumulated from 3 independent experiments.

(D) Corrected fluorescence intensity levels of anti-nitrotyrosine antibody confocal z-stacks of dominant active Hif-1α (DA1) injected embryos in the presence or absence of Mm infection at 1dpi. Control morpholino is shown in the clear bars and il-1 morpholino (il-1 MO) in the filled bars. Data shown are mean ± SEM, n=54-59 cells from 10-12 embryos accumulated from 3 independent experiments.

Figure 6. Hif-1α stabilisation leads to upregulation of *il-1β* and increased neutrophil nitric oxide production that is protective against infection.

During normal (control) Mm infection Hif-1α, Il-1β and NO transcript levels rise after infection, but are not sufficient to control infection (Elks *et al*, 2013). When Hif-1α is stabilised, Il-1β and subsequent neutrophil NO upregulation occurs in the absence of

734 infection, priming the immune response to better deal with infection leading to lower
735 burden.
736
737 **Figure S1. *TgBAC(il-1β:GFP)sh445* recapitulates *il-1β* wholemount *in situ***
738 **hybridisation pattern following sterile tailfin transection.**
739 (A) Wholemount *in situ* hybridisation of *il-1β* in tailfin injured 2dpf embryos.
740 (B) Fluorescent confocal micrographs of *TgBAC(il-1β:GFP)sh445* expression after
741 tailfin injury. Upper and lower panels show the same individual embryo 0 and 12hpi.
742 (C) Fluorescent confocal micrographs of *TgBAC(il-1β:GFP)sh445* crossed to
743 *Tg(lyz:Ds- RED2)nz50* labelling neutrophils at 1 hour post wound (1hpw) and 6hpw.
744
745
746 **Figure S2. CRISPR-Cas9 *il-1β SH446* mutant.**
747 (A) Screenshot of Ensembl zebrafish *il-1β* coding sequence with CRISPR-Cas9
748 target indicated in the fourth exon.
749 (B) DNA alignment of WT *il-1β* sequence and *il-1βSH446* showing the 44 base pair
750 deletion caused by CRISPR-Cas9.
751 (C) Amino acid alignment of WT *il-1β* sequence and *il-1βSH446* with arrowhead
752 showing the premature stop and removal of the putative Il-1β cleavage site.
753 (D) Sequencing trace showing position of CRISPR-Cas9 induced deletion.
754
755
756
757 **Figure S3. Anti-nitrotyrosine signal is predominantly found in neutrophils after**
758 **Mm infection.**

(A) Example fluorescence confocal z-stacks of the caudal vein region of *Tg(mpx:GFP)i114* embryos (green neutrophils) stained with Alexa-633 labelled anti-nitrotyrosine antibody (cyan), imaged at 1dpi in the presence of Mm mCherry infection (red).

Supplemental Movie 1. *Il-1β:GFP* expression in activated immune cells after Mm infection.

(A) Fluorescent confocal videotimelapse of *il-1β:GFP* in immune cells containing Mm infection (*il-1β:GFP* in green and Mm mCrimson in red).

Figure 1

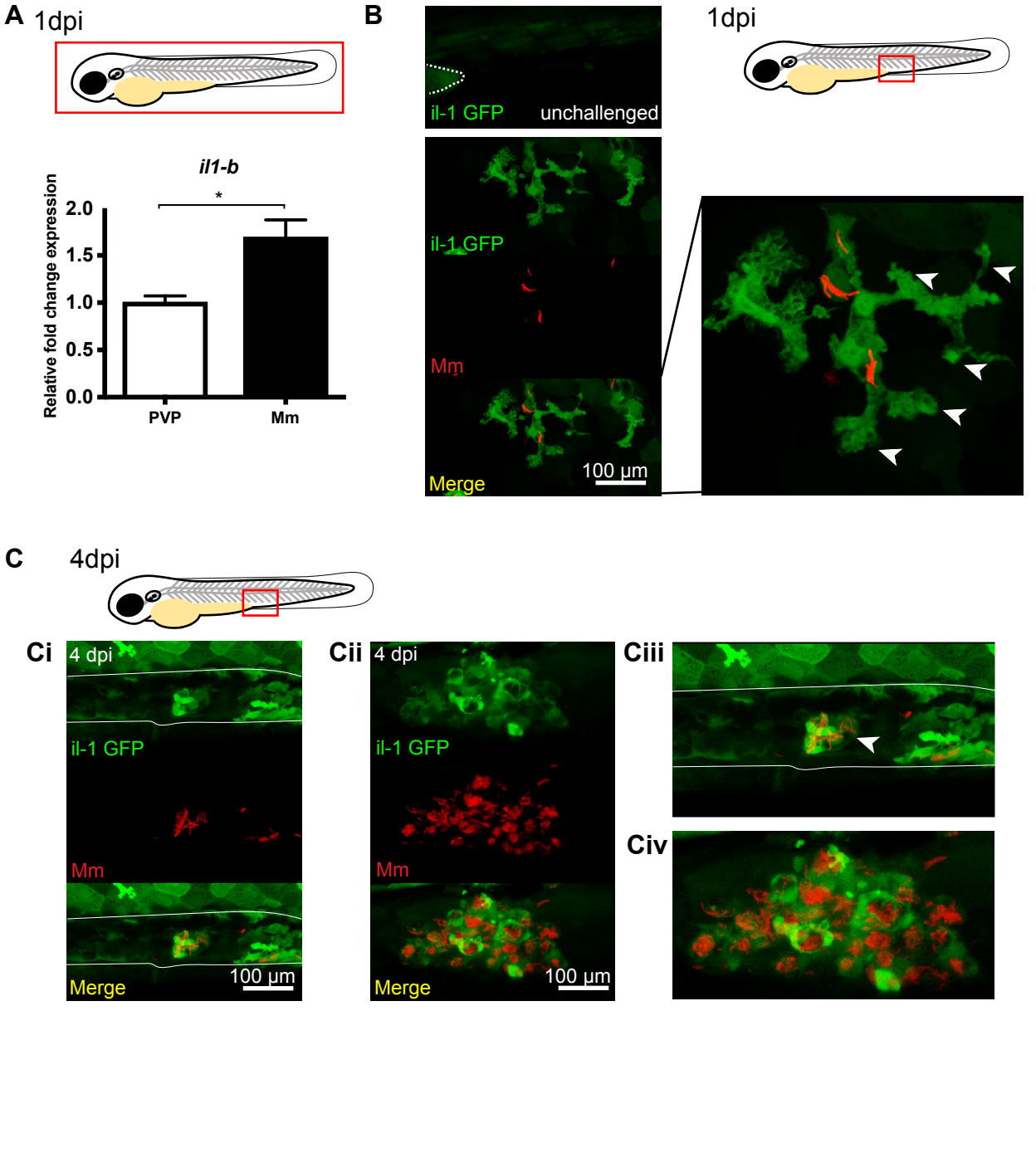
A
1dpi
il1-b
*
Relative fold change expression
2.0
1.5
1.0
0.5
0.0
PVP
Mm
B
il-1 GFP
unchallenged
1dpi
il-1 GFP
Mm
Merge
100 µm
C
4dpi
Ci
4 dpi
il-1 GFP
Mm
Merge
100 µm
Cii
4 dpi
il-1 GFP
Mm
Merge
100 µm
Ciii
Civ

Figure 2

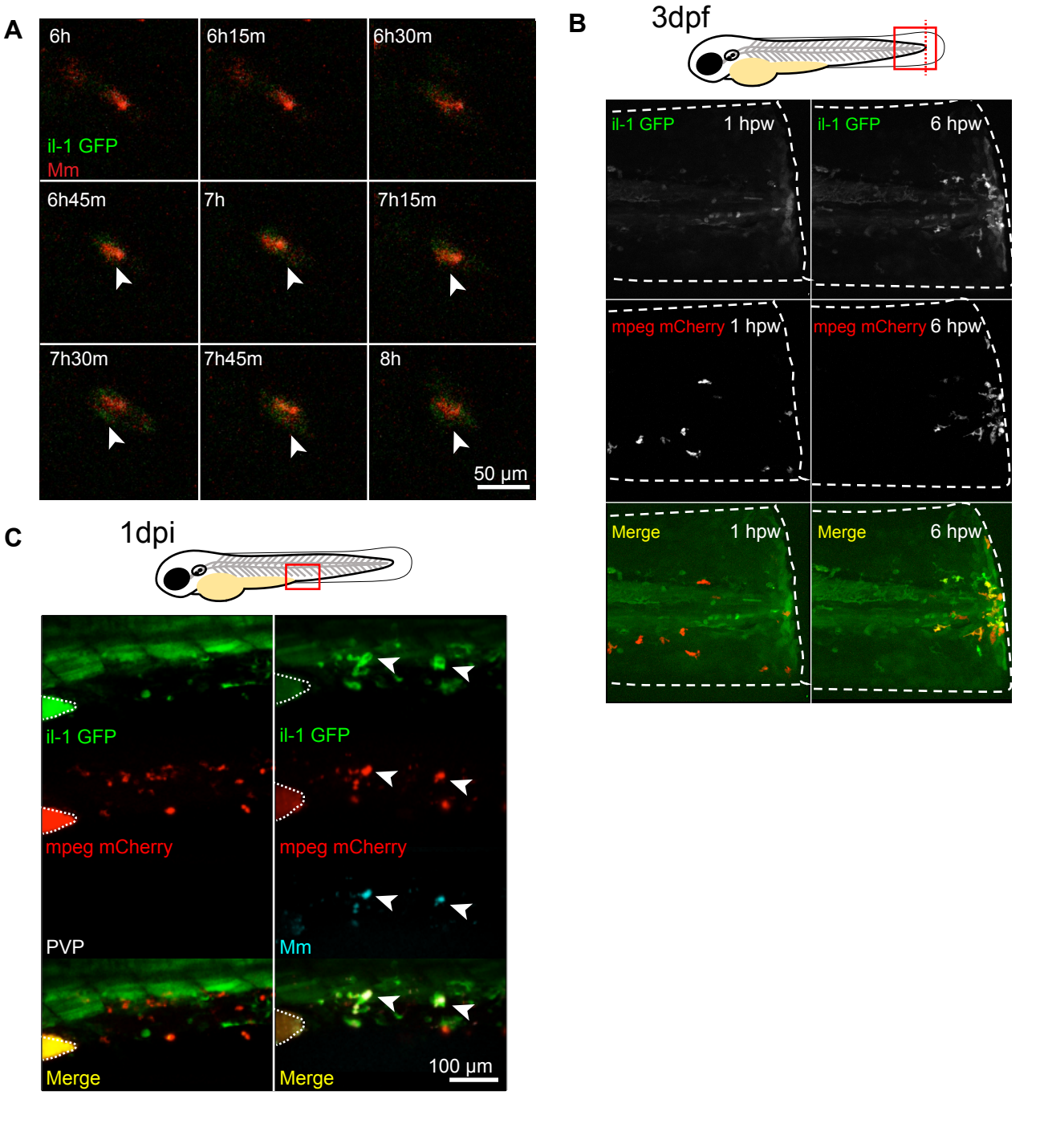
A
6h
6h15m
6h30m
il-1 GFP
Mm
6h45m
7h
7h15m
7h30m
7h45m
8h
50 µm
B
3dpf
il-1 GFP 1 hpw
il-1 GFP 6 hpw
mpeg mCherry 1 hpw
mpeg mCherry 6 hpw
Merge 1 hpw
Merge 6 hpw
C
1dpi
il-1 GFP
mpeg mCherry
PVP
il-1 GFP
mpeg mCherry
Mm
Merge
Merge
100 µm

Figure 3

A

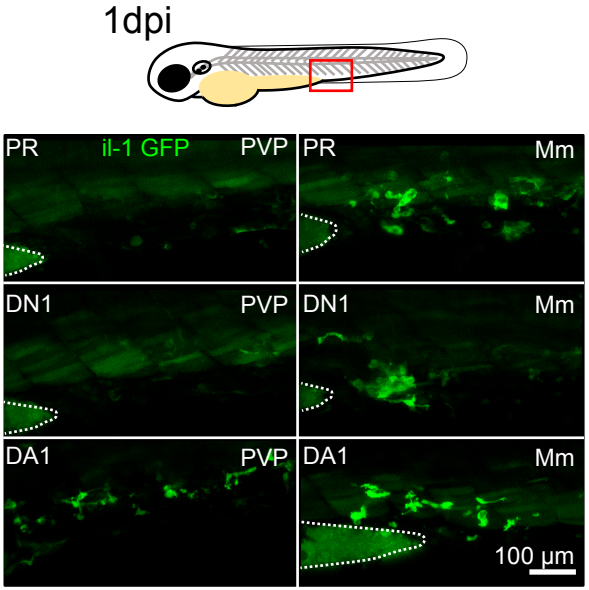
1dpi
PR
il-1 GFP
PVP
PR
Mm
DN1
PVP
DN1
Mm
DA1
PVP
DA1
Mm
100 µm

B

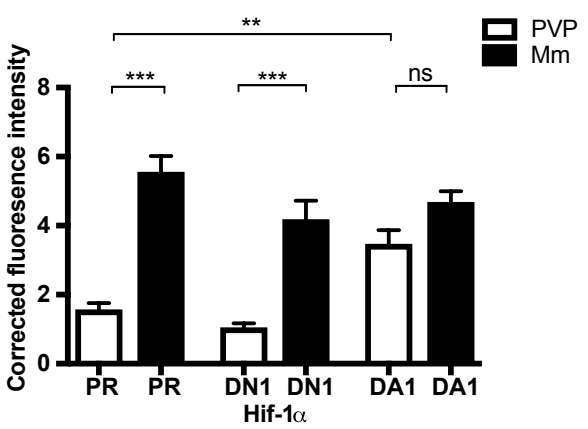
**
***
***
ns
PVP
Mm
Corrected fluoresence intensity
0
2
4
6
8
PR
PR
DN1
DN1
DA1
DA1
Hif-1α

Figure 4

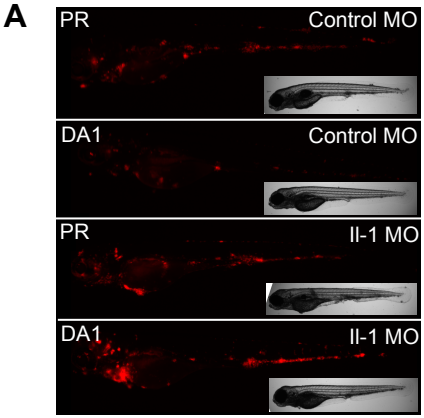
A
PR
Control MO
DA1
Control MO
PR
Il-1 MO
DA1
Il-1 MO

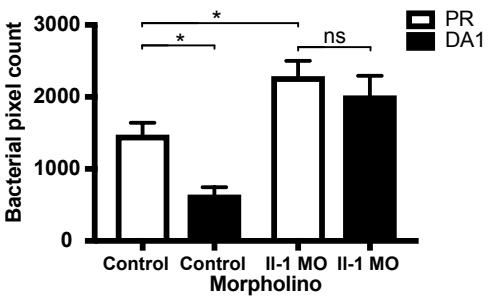
B
Bacterial pixel count
3000
2000
1000
0
*
*
ns
PR
DA1
Control
Control
Il-1 MO
Il-1 MO
Morpholino

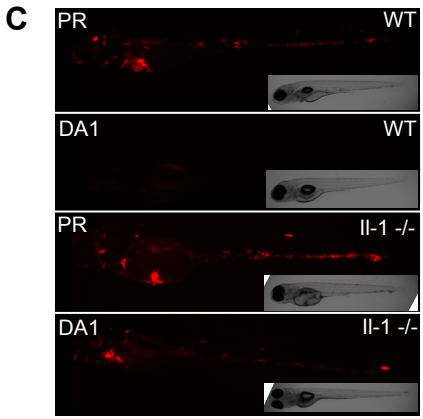
C
PR
WT
DA1
WT
PR
Il-1 -/-
DA1
Il-1 -/-

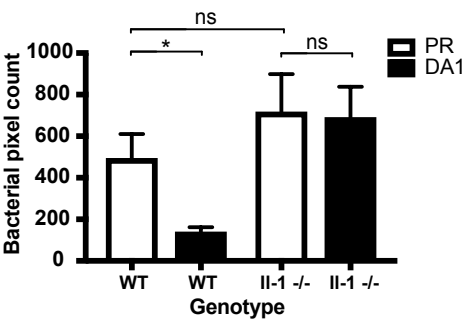
D
Bacterial pixel count
1000
800
600
400
200
0
ns
*
ns
PR
DA1
WT
WT
Il-1 -/-
Il-1 -/-
Genotype

Figure 5

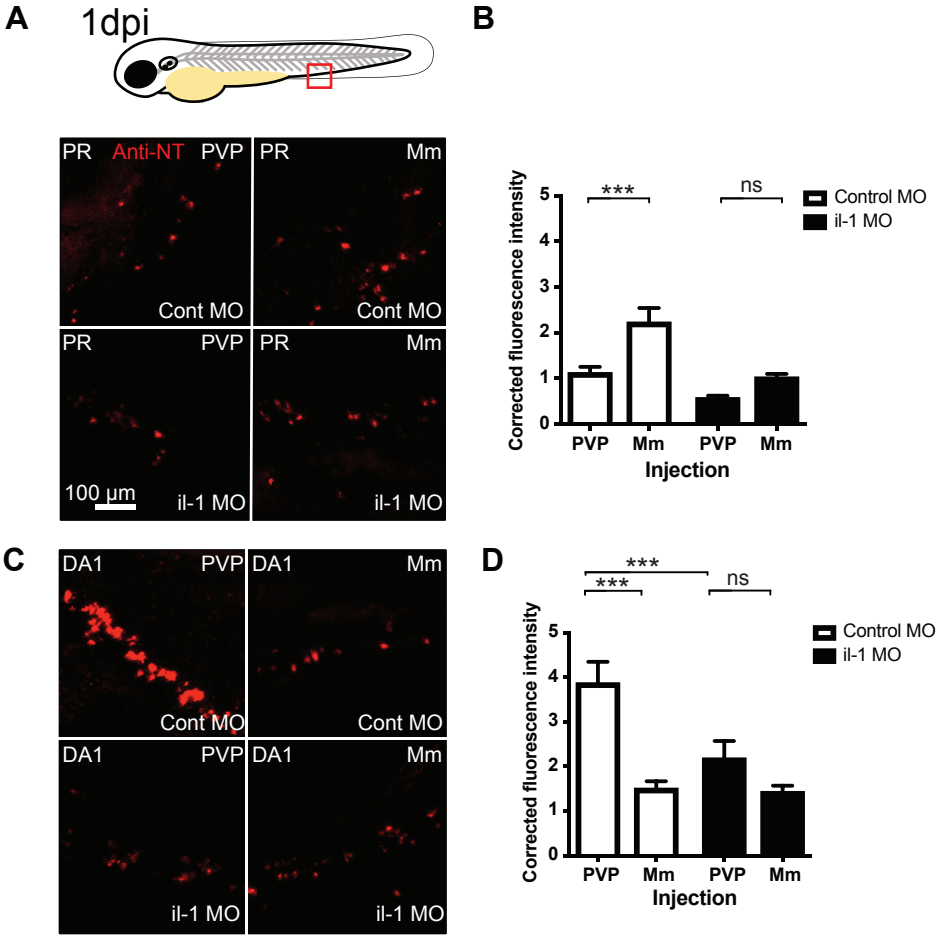
A
1dpi
PR Anti-NT PVP
PR Mm
Cont MO
Cont MO
PR PVP
PR Mm
100 µm
il-1 MO
il-1 MO
B
Corrected fluorescence intensity
***
ns
Control MO
il-1 MO
0
1
2
3
4
5
PVP Mm PVP Mm
Injection
C
DA1 PVP
DA1 Mm
Cont MO
Cont MO
DA1 PVP
DA1 Mm
il-1 MO
il-1 MO
D
***
***
ns
Corrected fluorescence intensity
Control MO
il-1 MO
0
1
2
3
4
5
PVP Mm PVP Mm
Injection

Figure 6

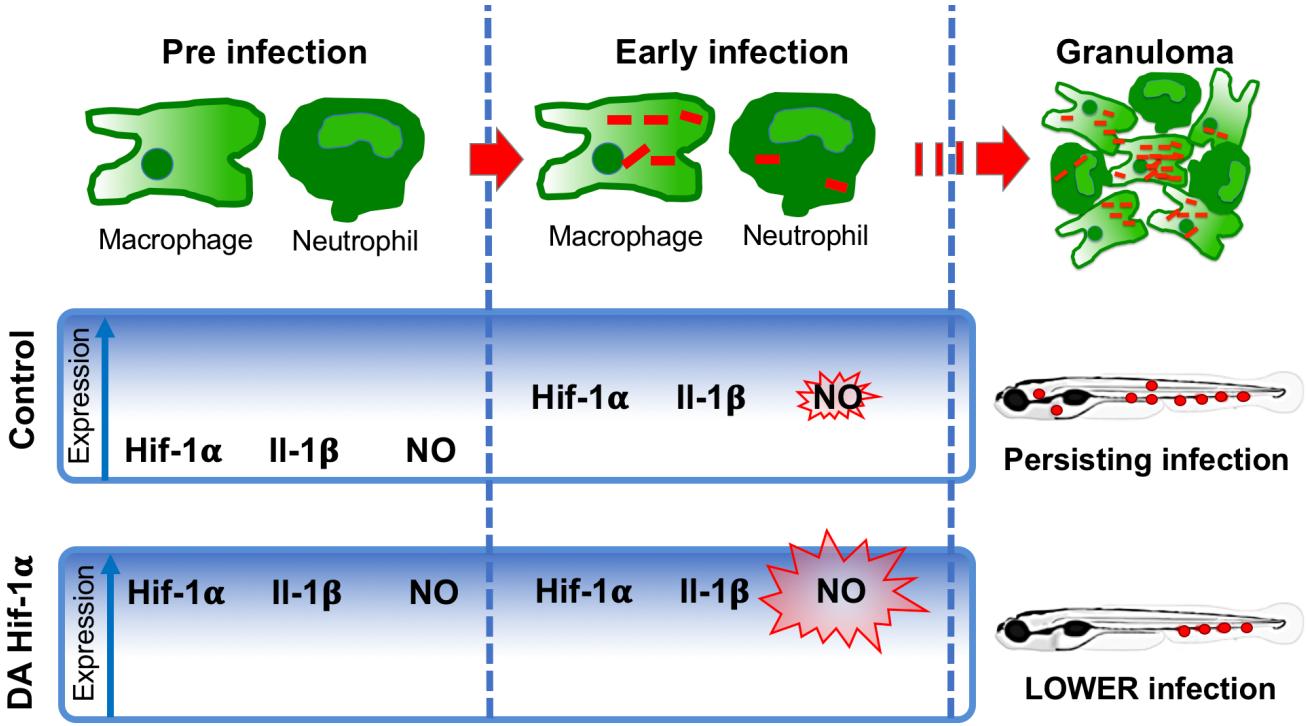
Pre infection
Early infection
Granuloma
Macrophage
Neutrophil
Macrophage
Neutrophil
Control
Expression
Hif-1α
Il-1β
NO
Hif-1α
Il-1β
NO
Persisting infection
DA Hif-1α
Expression
Hif-1α
Il-1β
NO
Hif-1α
Il-1β
NO
LOWER infection